International Journal of Latest Research in Engineering and Technology (IJLRET)
ISSN: 2454-5031
www.ijlret.com || Volume 11 - Issue 08 || August 2025 || PP. 45-50

A Transient Stability Analysis of Sensorless Control for IPMSM

Dr. Dongwoo Lee[1]
[1]*Assistant Professor, Department of Electrical & Control Engineering, Cheongju University, Korea*

Abstract: This study investigates the transient performance of sensorless control strategies for Interior Permanent magnet Synchronous Motors (IPMSMs), focusing on back-electromotive force (back-EMF) estimation techniques with Phase Locked Loop (PLL) type estimator. The stability of gain selection for each controller comprising the sensorless control algorithm was analyzed, with particular focus on ensuring reliable operation during both acceleration and deceleration phases of motor speed variation. The proposed controller design methodology was validated through simulation, confirming the effectiveness of gain tuning and the robustness of the sensorless control system under transient conditions.

Keywords: IPMSM, PLL type estimator, transient state stability

1. Introduction

Permanent Magnet Synchronous Motors (PMSMs) have become prevalent in precision control applications, attributed to their compact structure and high conversion efficiency. The literature highlights IPMSMs as a promising topology, owing to their ability to achieve high torque through the synergistic effect of magnetic and reluctance torque [1]. Sensorless control techniques for PMSMs have also gained popularity, offering advantages such as enhanced reliability, reduced system cost, and simplified mechanical design.

Achieving high-performance sensorless control requires accurate estimation of rotor position and speed. Two primary approaches are commonly used for this purpose. one relies on the back-EMF generated during motor operation to facilitate sensorless control [2], while the other utilizes high-frequency voltage injection, extracting rotor position information from the resulting current response of motor [3].

Numerous estimation algorithms have been proposed to derive back-EMF and rotor position, including state observers such as the Kalman filter, sliding mode observers, and physical models like the phaselocked loop (PLL). However, back-EMF amplitude becomes negligible at very low speeds or standstill, even when accurately estimated, limiting its effectiveness in such conditions. To address this limitation, high-frequency signal injection methods have been introduced as a more robust alternative for low-speed operation. Nevertheless, these methods inherently produce audible noise and additional power losses due to the injected signals. Moreover, in PMSMs lacking spatial inductance saliency, injection-based techniques are not applicable for sensorless control.The transition between back-EMFbased and injection-based estimation is typically determined through experimental analysis, often defined as the speed range where both methods yield reliable results [4]–[7].

This paper focuses on the transient-state behavior of sensorless control systems based on an extended EMF model formulated in the rotor reference frame. The primary objective is to establish a systematic method for selecting control parameters that ensure stable motor operation during dynamic conditions. Specifically, the parameters associated with back-EMF estimation and PLL-type observers must be chosen to maintain stability and enable rapid dynamic response. To facilitate this, a mathematical model of the IPMSM incorporating extended EMF is utilized to estimate rotor position and speed. The extended EMF is derived using a disturbance observer, while the rotor position error is obtained via a PLL-type estimator. To evaluate the transient performance, simulation results are presented under various control parameter configurations.

2. Mathematical Model of IPMSMs

Fig. 1 shows a space vector diagram for a PMSM [5]. Theα-β and d-q axis represent the stationary and the rotor reference frames, respectively. The γ-δ axis is an estimated frame used in vector control for sensorless.The IPMSMs voltage equation in the d-q axis can be described through the following:

International Journal of Latest Research in Engineering and Technology (IJLRET)
ISSN: 2454-5031
www.ijlret.com || Volume 11 - Issue 08 || August 2025 || PP. 45-50

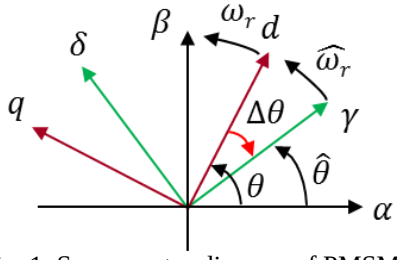

Fig. 1: Space vector diagram of PMSM.

$$\begin{bmatrix} V_d \\ V_q \end{bmatrix} = \begin{bmatrix} R + pL_d & -\omega_r L_q \\ \omega_r L_d & R + pL_q \end{bmatrix} \cdot \begin{bmatrix} i_d \\ i_q \end{bmatrix} + \begin{bmatrix} 0 \\ \omega_r \phi_m \end{bmatrix} \tag{1}$$

To simplify the analytical modeling of the interior permanent magnet synchronous motor (IPMSM), the extended electromotive force (EMF) formulation can be incorporated into the rotor reference frame as follows:

$$\begin{bmatrix} V_\gamma \\ V_\delta \end{bmatrix} = \begin{bmatrix} R + pL_d & -\omega_r L_q \\ \omega_r L_q & R + pL_d \end{bmatrix} \cdot \begin{bmatrix} i_\gamma \\ i_\delta \end{bmatrix} + \omega_r \lambda_{PM} \begin{bmatrix} -\sin \Delta\theta \\ \cos \Delta\theta \end{bmatrix} + (\hat{\omega}_r - \omega_r) L_d \begin{bmatrix} -i_\delta \\ i_\gamma \end{bmatrix} \tag{2}$$

The estimated rotor position error$\Delta\hat{\theta}$can be calculated using (3):

$$\Delta\hat{\theta} = tan^{-1}\left(\frac{-E_{ex} \cdot sin\ \Delta\theta}{E_{ex} \cdot cos\ \Delta\theta}\right) = -\tan^{-1}\left(\frac{\hat{e}_\gamma}{\hat{e}_\delta}\right) \tag{3}$$

3. Disturbance Observer Design for Back-EMF Estimation

The equivalent block diagram of disturbance observer for estimation of extended EMF of γ-axis isshown in Fig. 2. The $g_\gamma$represents the designed bandwidth of the back-EMF estimator. And the disturbance observer incorporates a differential operator to obtain the reverse model of the system. To mitigate the adverse effects associated with differentiation, such as amplification of high-frequency noise, the back-EMF estimator is equipped with both low-pass and high-pass filters. Therefore, optimizing observer gain is critical for enhancing transient response and minimizing harmonic distortion. The g_γ of the disturbance observer is assigned under taking two considerations account. One is a robustness of the extended EMF estimation against speed estimation error. The other is for suppression of harmonic components in back-EMF.

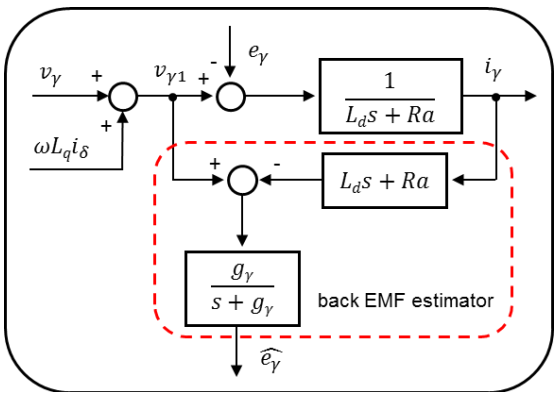

Fig. 2: Back-EMF estimator using disturbance observer.

The parameter g_γ can be decided by manual tuning for robust estimation. It is also noteworthy that the bandwidth of the current control loop exceeds that of the speed control loop. Consequently, the observer filter bandwidth must be sufficiently large to ensure accurate state estimation and maintain system stability.In general, the conventional system is set as g_γ = 600 rad/s.

4. PLL-Type Estimator Design for Speed and Position Estimation

Regarding the stable bandwidth selection of PLL-type estimator, Reference [4] outlines foundational principles for bandwidth tuning method.

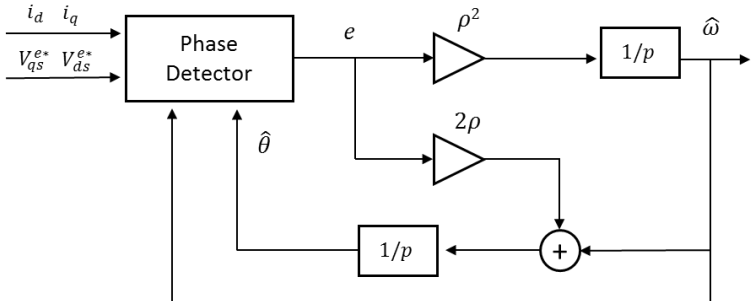

Fig. 3: Flowchart of the PLL-type estimator.

$$\begin{bmatrix} \dot{\tilde{\omega}}_r \\ \dot{\tilde{\theta}}_r \end{bmatrix} = \begin{bmatrix} 0 & -\rho^2 \\ 1 & -2\rho \end{bmatrix} \cdot \begin{bmatrix} \tilde{\omega}_r \\ \tilde{\theta}_r \end{bmatrix} \tag{4}$$

From (4), The system matrix is found as

$$A = \begin{bmatrix} 0 & -\rho^2 \\ 1 & -2\rho \end{bmatrix} \tag{5}$$

From (5), the characteristic polynomial c(s) is found as

$$c(s) = det(sI - A) = (s+\rho)^2 = s^2 + s \cdot 2\rho + \rho^2 \tag{6}$$

Where I is the identity matrix and ρ is estimator bandwidth. As the control system poles are the roots of c(s), the two poles which both located at s = $-\rho$ yield a stable system without oscillatory behavior. Moreover, the system poles exhibit a clear dependency on rotor speed, which directly influences the dynamic response of the position controller. Regarding the selection of the closed-loop bandwidth of current controller, a rule of thumb is thatthe observer poles are typically selected to be at least ten times greater than the parameter ρ, in order to prevent performance degradation of the estimator.And the ρ must have larger value than speed controller bandwidth.In Fig. 4. The speed and position estimator employed in this study is based on the phaselocked loop (PLL) structure, as introduced in [7].

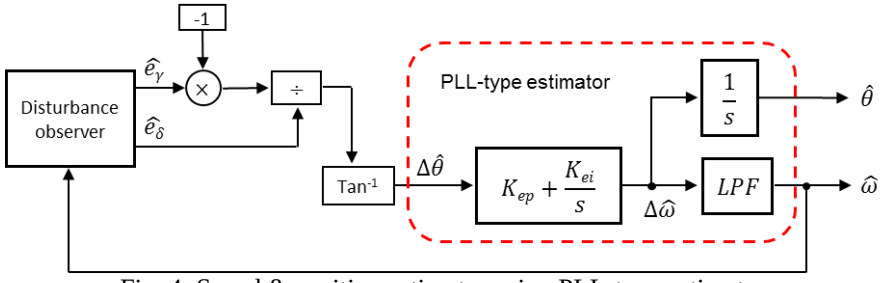

Fig. 4: Speed & position estimator using PLL-type estimator.

The back-EMF signals estimated in rotor reference frame can be converted into estimated rotor position error$\Delta\hat{\theta}$. To sensorless control simulation, the gains of the PI controller using PLL-type estimator can be used. The design of the characteristic polynomial is below:

$$s^2 + 2\varsigma\omega_n s + \omega_n^2, k_{ep} = 2\varsigma\omega_n, k_{ei} = \omega_n^2 \tag{7}$$

where ζ is damping radio and the ω_n is natural frequency.From (13), The current controller bandwidth can be defined as$\rho = \varsigma\omega_n$

5. Simulation results

The configuration of the simulation system is illustrated in Fig. 5. The PLL-type estimator calculates the rotor position and speed based on the observed back-EMF signals. To validate the accuracy of the estimated information, the results are compared with actual rotor angle and speed obtained from resolver output signals.The sensorless control strategy for IPMSMs was implemented and validated through PSIM simulations. The sensorless control architecture is illustrated in Figure 5. Also, IPMSM parameters is listed in Table 1.

Table 1: IPMSM parameters

Parameter	Value
Number of poles	6
Rated Speed	1600 rpm
Stator resistance	90 mΩ
d-axis Inductance	2.51 mH
q-axis Inductance	6.94 mH
Back-EMF constant	128 V/krpm
Rotor inertia	0.001 kg-m^2
Mechanical time constants	0.01 s

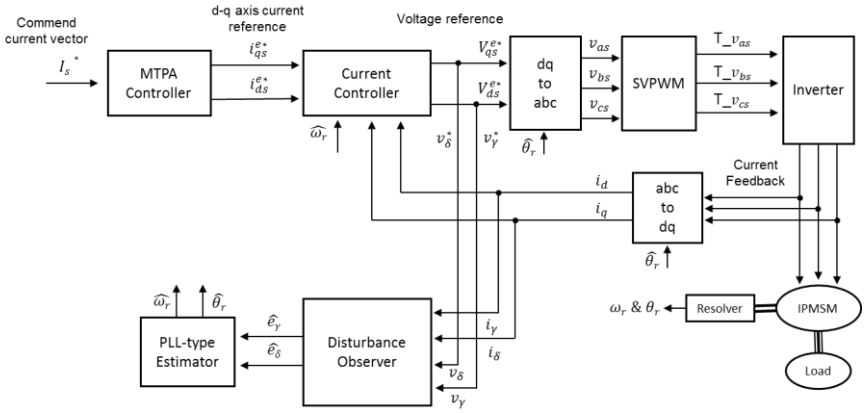

Fig. 5. Functional block diagram of the sensorless control included PLL-type estimator for simulation.

In Fig. 6,the stable region is below 377rad/s according to (7) and the damping radio is limited as 0.5 ≤ζ≤ 5 and natural frequency is limited as 50 ≤ω_n≤ 400rad/s for the simulation.

		Damping radio [ζ]										
Natural frequency [ω_n]		1	2	3	4	5	6	7	8	9	10	11
rad/s		0.5	0.7071	1	1.5	2	2.5	3	3.5	4	4.5	5
1	50	25	35	50	75	100	125	150	175	200	225	250
2	100	50	71	100	150	200	250	300	350	400	450	500
3	150	75	106	150	225	300	375	450	525	600	675	750
4	200	100	141	200	300	400	500	600	700	800	900	1000
5	250	125	177	250	375	500	625	750	875	1000	1125	1250
6	300	150	212	300	450	600	750	900	1050	1200	1350	1500
7	350	175	247	350	525	700	875	1050	1225	1400	1575	1750
8	400	200	283	400	600	800	1000	1200	1400	1600	1800	2000

Fig. 6: The stable region of PLL-type estimator.

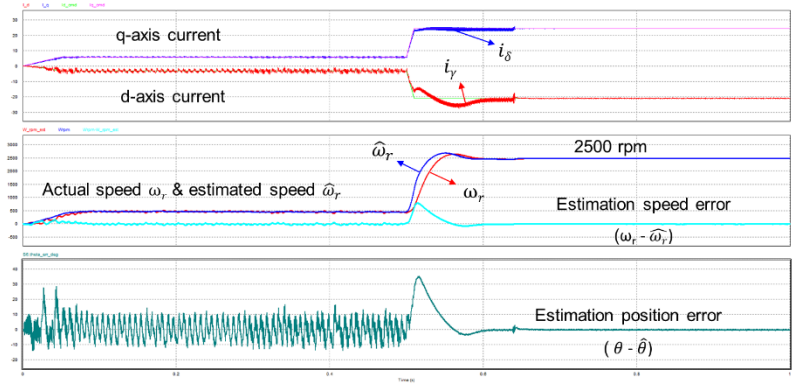

Fig. 7: Estimation speed error in transient state (500rpm→2500rpm).

Considering the stable region, the simulation on step response runs to find the difference value between actual and estimated speed. In Fig. 7. The simulation results show estimation speed, position and error of one

test point in the transient state responses (ζ = 1, ω_n = 200rad/s). Note also that the control algorithm only used current control. So, the motor speed is decided the output torque with the load.

Fig. 8 shows the maximum estimation speed error in the transient state according to the speed, damping radio and natural frequency. The stable operating point is decreased as the motor speed is increased. And the estimation speed error is increased.

		Damping radio [ζ]										
Natural frequency [ω_n]		1	2	3	4	5	6	7	8	9	10	11
rad/s		0.5	0.7071	1	1.5	2	2.5	3	3.5	4	4.5	5
1	50											
2	100								835.46	829.86	810.25	815
3	150					827.1	815.84	790.97	790.25	782.94		
4	200	848.93	834.99	825.13	817.85	789.6	780.02					
5	250	831.24	802.94	792.87	737.82	776.7						
6	300	803.84	777.57	746.83	737.06							
7	350	766.02	730.03	738.79								
8	400	732.27	700.19	735.07								

Fig. 8: Estimation speed error in transient state (500rpm→2500rpm).

Therefore, the stable operation is possible by selecting overlap point both of low and high speed. For example, In Fig. 9. The simulation result presents stable operation from 500rpm to 2500rpm by overlap operating point between Fig. 6 and Fig. 8(ζ = 1, ω_n = 200rad/s). But, at a more low operating point(ζ = 1, ω_n = 150rad/s), the control system is unstable in Fig. 10. Because the operating point is in an unstable area at the moment of acceleration in Fig. 8.

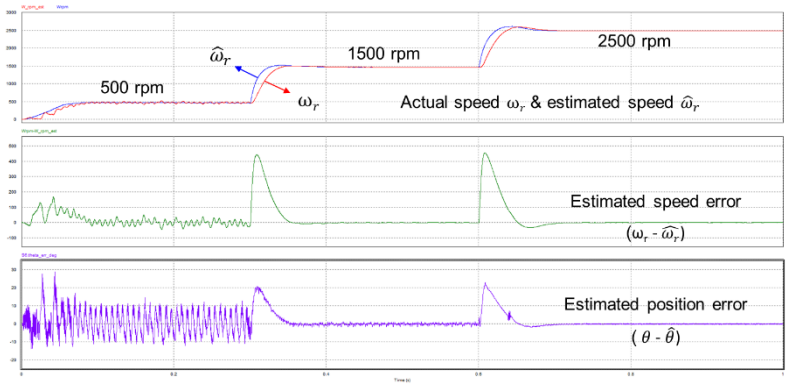

Fig. 9: Step response (500rpm → 1500rpm → 2500rpm) withoverlap operating point (ζ = 1, ω_n = 200rad/s).

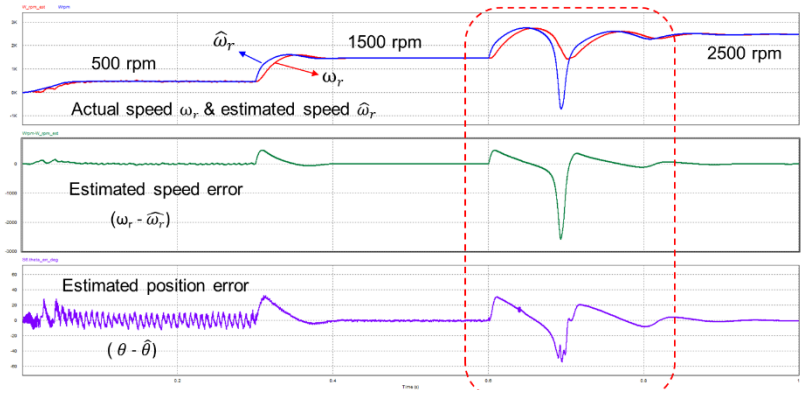

Fig. 10: Step response (500rpm → 1500rpm → 2500rpm) withoverlap operating point (ζ = 1, ω_n = 150rad/s).

6. Conclusion

This paper presents a robust bandwidth selection strategy for a phase-locked loop (PLL)-based estimator used in sensorless control of interior permanent magnet synchronous motors (IPMSMs), enabling accurate estimation of rotor speed and position. Additionally, a controller design methodology is proposed to ensure system stability during transient events caused by speed variations. Simulation results obtained using PSIM confirm that the proposed approach enables reliable sensorless operation of IPMSMs under dynamic conditions.

References

[1] P. Pillay and R. Krishnan, Application characteristics of permanent magnet synchronous and brushless dc motors for servo drives, *in Conf. Rec. IEEE-IAS Annu. Meeting, 3*, 2000, 1814-1819.

[2] S. Morimoto, K. Kawamoto, M. Sanada and Y. Takeda, Sensorless control strategy for salient-pole PMSM based on extended EMF in rotating reference frame, *IEEE Trans. Ind. Applicat., 38*, 2002, 1054-1061.

[3] J.-H. Jang, S.-K. Sul, J.-I. Ha, K. Ide, and M. Sawamura, Sensorless drive of SMPM motor by high frequency signal injection, *in Proc. IEEE APEC'02, 1*, 2002, 279-285.

[4] Oskar Wallmark, and Lennart Harnefors, Sensorless Control of Salient PMSM Drives in the Transition Region, *IEEE Trans. Ind. Elec., 53(4)*, 2006, 1179-1187.

[5] T. Aihara, A. Toba, T. Yanase, A. Mashimo, and K. Endo, Sensorless torque control of salient-pole synchronous motor at zero-speed operation, *IEEE Trans. Power Electron., 14(1)*, 1999, 202-208.

[6] Oskar Wallmark, Lennart Harnefors, and Ola Carlson, An Improved Speed and Position Estimator for Salient Permanent-Magnet Synchronous Motors, *IEEE Trans. Power Electron., 52(1)*, 2005, 255-262.

[7] Lennart Harnefors and Hans-Peter Nee, A General Algorithm for Speed and Position Estimation of AC Motors, *IEEE Trans. Ind. Elec., 47(1)*, 2000, 77-83.

[8] K.-W. Lee and J.-I. Ha, Evaluation of back-EMF estimators for sensorless control of permanent magnet synchronous motors, *J. Power Electron., 12(4)*, 2012, 604-614.